Article

Seasonal Evolution of the Chemical Composition of Atmospheric Aerosol in Terra Nova Bay (Antarctica)

Flavio Vagnoni [1] , Silvia Illuminati [1,*], Anna Annibaldi [1,*] , Francesco Memmola [1], Giada Giglione [1] , Anna Maria Falgiani [1,2], Federico Girolametti [1] , Matteo Fanelli [1], Giuseppe Scarponi [1] and Cristina Truzzi [1]

1   Department of Life and Environmental Sciences, Università Politecnica delle Marche, Via Brecce Bianche, 60131 Ancona, Italy; f.vagnoni@univpm.it (F.V.); f.memmola@univpm.it (F.M.); g.giglione@pm.univpm.it (G.G.); a.falgiani@pm.univpm.it (A.M.F.); f.girolametti@pm.univpm.it (F.G.); matteo.fanelli@virgilio.it (M.F.); g.scarponi@univpm.it (G.S.); c.truzzi@univpm.it (C.T.)
2   Regional Agency for Environmental Protection (ARPA), 63100 Ascoli Piceno, Italy
*   Correspondence: s.illuminati@univpm.it (S.I.); a.annibaldi@univpm.it (A.A.); Tel.: +39-071-2204981 (S.I. & A.A.)

Abstract: Atmospheric aerosol samples were collected at Faraglione Camp, 3 km away from the Italian Mario Zucchelli Station (Terra Nova Bay, Ross Sea), from 1 December 2013 to 2 February 2014. A two-step extraction procedure was applied to characterize the soluble and insoluble components of PM_{10}-bound metals. Samples were analyzed for Al, Fe, Cd, Cu, and Pb by square wave anodic stripping voltammetry (SWASV) and by graphite furnace atomic absorption spectrophotometer (GF-AAS). The mean atmospheric concentrations were (reported as means $\pm$ SD) Al 24 ± 3 ng m^{-3}; Fe 23 ± 4 ng m^{-3}; Cd 0.92 ± 0.53 pg m^{-3}; Cu 43 ± 9 pg m^{-3}, and Pb 16 ± 5 pg m^{-3}. The fractionation pattern was metal-specific, with Al, Fe, and Pb mainly present in the insoluble fractions, Cd in the soluble one, and Cu equally distributed between the two fractions. The summer evolution showed overall constant behavior of both fractions for Al and Fe, while a bell-shaped trend was observed for the three trace metals. Cd and Cu showed a bell-shaped evolution involving both fractions. A seasonal increase in Pb occurred only for the insoluble fraction, while the soluble fraction remained almost constant. Sequential extraction and enrichment factors indicated a crustal origin for Al, Fe, and Pb, and additional (marine or anthropogenic) contributions for Cd and Cu. Back trajectory analysis showed a strong contribution of air masses derived from the Antarctic plateau. A potential low contribution from anthropized areas cannot be excluded. Further studies are necessary to better characterize the chemical composition of the aerosol, to discriminate between natural and anthropogenic sources, and to evaluate a quantitative source apportionment.

Keywords: sequential extraction procedure; metals; Antarctic aerosol; seasonal evolution; enrichment factors

1. Introduction

Atmospheric aerosol is the primary source of soluble or insoluble solid and liquid material that, in different ways, plays a key role in the terrestrial climate system [1]. Particulate matter released in the atmosphere, from natural or anthropogenic sources, affects the solar radiation transfer, interacts with cloud formation and controls the optical, electric, and radiative properties of the atmosphere [2]. The environmental effects of aerosols depend on their atmospheric concentration, particle size, and chemical composition. Atmospheric aerosol can be transported from other continents in remote areas, for example, polar regions, through long-range atmospheric transport (LRAT), a phenomenon that is mainly controlled by wind and meteorological conditions [3,4].

Antarctica, as it is situated far from anthropogenic pollution sources, is the ideal place to study natural processes, like those related to aerosol. Polar regions are the most sensitive areas to changes in the climate because of their high albedo, the sea ice extent and

persistence, and their role in controlling atmospheric and marine circulation patterns [5]. The literature data suggest that Antarctica acts as a trap for atmospheric particulate matter (APM) and related airborne pollutants (metals, pesticides, hydrocarbons, and persistent organic pollutants) that reach the polar regions via LRAT from other continents [3].

Apart from major constituents, only limited trace element measurements have been carried out on the Antarctic aerosol samples [6–14]. However, the scientific community has recently recognized the need for a better physical–chemical characterization of the composition of APM—with a particular focus on the trace element content—because of their potentialities to be used as tracers of different emission sources [15,16]. In fact, besides the well-known Na, Mg, K, and Ca as markers of primary marine aerosol sources [15], or sulfates and ammonium used to detect marine biogenic sources [15,17], several trace elements (Al, La, Ce, Nd) can be employed as valuable indicators of crustal inputs (i.e., soils or mineral dust) [16]. Furthermore, metals such as As, Pb, Cd, Cr, and Ni are tracers of anthropogenic pollution, in relation to atmospheric emissions [4,10,13]. The investigation of the chemical composition of the Antarctic atmosphere is one of the key points in polar research. Indeed, the distance from anthropogenic and continental emission sources makes Antarctica the leading natural laboratory in the world to study and investigate the cycles and movements of several elements and compounds, transformations of chemical species, and long-range transport from anthropized areas [14].

Metals in the environment are bound to several fractions exhibiting different bioavailability, toxicity, and mobility [18]. The labile fraction of the particle-bound metals is more readily available to the organisms, and hence, has a greater environmental risk than the residual fraction [19]. At the same time, different fractions can have different origins. Therefore, the determination of the total particle-bound metal content alone is not sufficient to assess the overall pollution and hazard levels and to completely understand the local and long-range transport mechanisms [20] since the effects of metals in the environment strongly depend on the chemical associated with the solid matrix [21].

Although time-consuming, chemical fractionation, in addition to particle size distribution, can be a valuable tool to assess biological and physicochemical availability, mobilization, metal accumulation, pollution, source apportionment, and transport mechanisms [11,21–24]. Several sequential chemical fractionation schemes have been reported in the literature for APM. Many of these are based on the sequential extraction procedure reported by Tessier et al. [25], the BCR sequential extraction procedure from the Bureau of References of the European Community [26], Chester's procedure [27], Zatka's procedures [28], and the procedure reported by Kyotani and Iwatsuki [29]. Several studies about the application of these extracting schemes or their successive adaptions to APM samples have been reported for many locations around the world [21,23,24,29], highlighting the key role of the mobile and residual fractions in eco-toxicological studies [30] and in the source traceability of APM [24]. Several extraction procedures providing only two fractions (soluble and insoluble ones) were developed over the years [24,31–33]. Generally, the most common extracting solution used in the sequential extraction of APM is deionized or ultrapure water since it is most representative of the natural solubility processes occurring in the environment [11,13,30,34–36]. Chemical fractionation of APM in polar regions is particularly challenging due to the low amount of PM that can be collected. Therefore, single or two-step extraction procedures have been generally preferred over the application of a multi-step scheme that could increase the risk of obtaining results below the detection limits [11,31,34]. In this study, we applied the sequential extraction procedure proposed by Kyotani and Iwatsuki [29]. This procedure was previously optimized in our laboratory to separate and determine the water-soluble, dilute HCl-extractable, and residual fractions of metals [11,33].

Here, we present a simplification of the method optimized to determine the water-soluble (below, simply "soluble") and the insoluble fractions of two minor constituents (Al and Fe) and three trace metals (Cd, Cu, and Pb) in the atmospheric aerosol over Terra Nova Bay (Victoria Land, Antarctica). To our knowledge, except for the studies of

Annibaldi et al. [11] and Truzzi et al. [33], no other surveys on metal fractionation have been reported from Antarctica.

Our principal goals were to (1) measure the concentrations Al, Fe, Cd, Cu, and Pb in one of the most remote areas of the world; (2) evaluate the metal partitioning between soluble and insoluble fractions; (3) characterize the summer evolution of the two metal fractions; (4) assess the natural and anthropogenic sources of the measured metal contents and the possible impact of long-range transport.

2. Materials and Methods

2.1. Laboratory, Apparatus, and Reagents

Clean room laboratories with areas in Class 5 (ISO 14644-1) (formerly Class 100, US Fed. Std. 209e) under laminar flow were used in both Antarctica and Italy [11,37,38]. Clean room garments, masks, and gloves were worn by the personnel, who strictly followed contamination control procedures during all the most critical treatments and sample analysis phases.

The Teflon-coated, high-volume PM10 sampler was from Analytica Strumenti (Air flow HVS-PM10-10EPA/EN, Pesaro, Italy, see Annibaldi et al. [11] for further details). The acid-cleaned 8″ × 10″ cellulose filters were from Whatman (Cat. No. 1441-866, thickness of 220 μm, ≤0.007% ashes, pore size of 20–25 μm, base weight of 85 g m^{-2}). The high-volume PM$_{10}$ sampler and the cellulose filters were decontaminated following a procedure previously developed [11]. The microwave (MW) accelerated reaction system MARS 5 (magnetron frequency of 2450 MHz) was from CEM (Matthews, NC, USA). The 100-mL HP-500 plus vessels for MW digestion were in Teflon PFA (perfluoroalkoxy copolymer) from CEM; more details of the MARS 5 were already reported by Illuminati et al. [36].

The Agilent DUO 240FS Atomic Absorption Spectrometer (GF-AAS), equipped with a graphite furnace (GTA120 Graphite Tube Atomizer) and a Zeeman-effect background corrector, was from Agilent (Santa Clara, CA 95051, USA). The voltammetric instrumentation, consisting of a 746 VA Trace Analyzer and a 747 VA Stand was from Metrohm (Herisau, Switzerland). It was equipped with a Teflon PFA cell and a three-electrode system, including an epoxy-impregnated graphite (Ultra Trace Graphite) rotating disk working electrode, an Ag/AgCl, KCl 3 mol l^{-1} reference electrode (to which all potentials are referred throughout), and a glassy carbon rod counter electrode.

Plastic containers, used for the storage of digested and not-digested sample solutions, were of low-density polyethylene (LDPE) material from Kartell, Italy. Variable-volume micropipettes and neutral tips were from Brand (Wertheim, Germany, Transferpette). LDPE bottles, Teflon digestion vessels, and all other plastic containers were decontaminated following the procedure reported elsewhere [36].

Ultrapure water was Milli-Q from Millipore (Bedford, MA, USA). Ultrapure HCl (34.5%, UpA), Ultrapure HNO$_3$ (70%, UpA), Superpure HCl (34–37%, SpA), Superpure H$_2$O$_2$ (ca. 30%, SpA) and Superpure HF (47–51%, SpA) were from Romil (Cambridge, UK). Atomic absorption standards for metals were from Merck (Darmstadt, Germany). Metal standard solutions were prepared every two weeks by direct dilution of stock solution standards using 5% HNO$_3$ acidified ultrapure water (for AAS determination) and 2:1000 HCl acidified ultrapure water (for voltammetric determination). Research-grade argon (≥99.998% purity) and nitrogen (≥99.999% purity) were from SOL SpA (Monza, Italy). The certified reference material SRM 1648a for trace metals in the urban particulate matter was from the National Institute of Standards and Technology (NIST).

2.2. Study Area

Aerosol samples were collected at Faraglione Camp (74.7161° S–164.1150° E), about 3 km south of the Italian Mario Zucchelli Station (MZS). MZS is a summer-based station and is operative from mid-October to the beginning of February. Consequently, research field activities can be performed only from November to the end of January. The study site is located 57 m above sea level and 250 m from the sea. Details of the site have been

reported elsewhere [11,37]. A map of the study site and the area around Mario Zucchelli Station are reported in Figure 1.
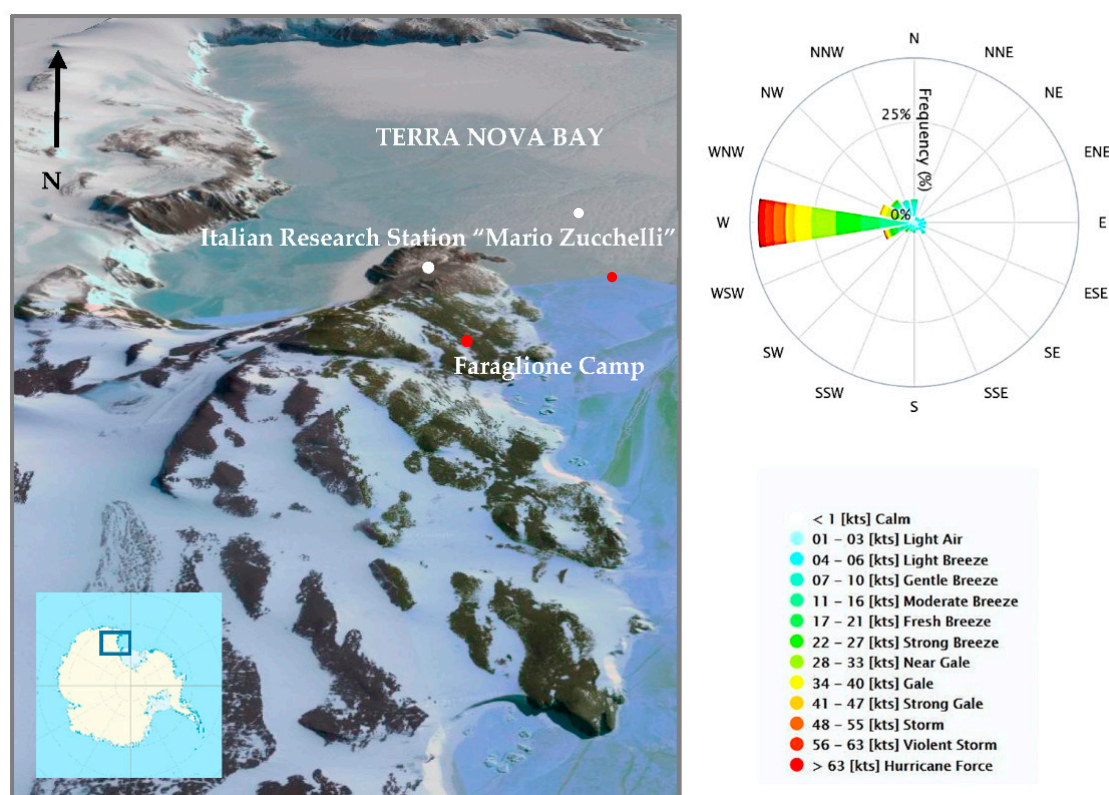

Figure 1. Map of Terra Nova Bay with the position of the sampling site (Faraglione Camp) and of the Italian Mario Zucchelli Station (MZS). The wind rose with the prevailing wind direction for the 2013–2014 Antarctic summer is also reported.

The Meteo-Climatological Observatory of the PNRA [39] produced daily means of the principal meteorological parameters (air temperature, relative humidity, ambient pressure, wind speed, and direction) at Faraglione Camp site (Figure 1). The Automated Weather Station (AWS) site close to the study area recorded the following values of the principal meteorological parameters; results are reported as the mean (minima ÷ maxima): temperature of $-3.0\,°C$ ($-10\,°C$ ÷ $+5.4\,°C$), pressure of 970 hPa (950 hPa ÷ 980 hPa), and relative humidity of 46% (18% ÷ 80%). The temperature and pressure increased during the summer; from mid-December, they showed stable high values until the end of the season (Figure 2a,c). The general trend of relative humidity (RH) remained almost constant during the sampling campaign (Figure 2b). The lowest RH values corresponded with the katabatic wind events over Terra Nova Bay (Figure 2d), as highlighted by the two variable graphs that are nearly specular. Until the beginning of January, the sampling site was subjected to strong surface winds, reaching speeds of ~20 m s^{-1} (~39 kts, Figure 2d), with gusts of 25–30 m s^{-1} (49−58 kts). Due to the strong katabatic effects, the most frequent surface wind direction was West (~40%) (see the wind rose plot in Figure 1).
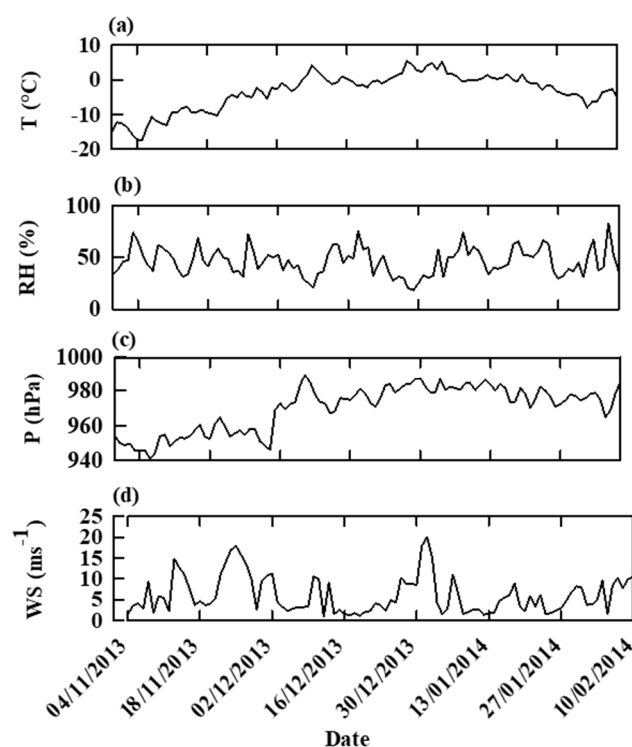
Figure 2. Meteorological parameter variations at Faraglione Camp during the sampling period. The panels (**a**–**d**) show the daily variation of air temperature (°C), relative humidity (%), pressure (hPa), and wind speed (m s^{-1}), respectively.

2.3. Sample Collection and Treatment

Six samples of atmospheric particulate matter were collected at Faraglione Camp from 1 December 2013 to 2 February 2014 using a high-volume impactor in combination with a 10 μm pre-separator (PM_{10}) and a volumetric control of air flux. The flow rate for the PM_{10} sampler was 1.13 m^3 min^{-1} ($\pm$10%) of standard air (298 K, 101.3 kPa). A sampling strategy of 10 days was adopted to comply with the requirements of trace element determination [11]. Before aerosol collection, the sampler was cleaned inside and outside by repeated washings using ultrapure water.

To check the background contamination, five blank filters ("field blanks" and "blanks as received") were also collected in the field approximately once every month. These were simply installed into the switched-off sampler for few minutes (about ten) and then treated as the sample filters. Sample and field blank filters were subdivided into two parts (to be used by different laboratories for different purposes). One-half of each filter was reserved for the present work. All these aliquots were stored in decontaminated 500 mL LDPE bottles at −20 °C until analysis.

An aliquot (1/8) of each original filter was subjected to a two-step extraction procedure previously set up [11,33] with 50 mL of ultrapure water for two days (the soluble fraction, Me$_{sol}$). The extract was then acidified with ultrapure HNO_3 (2 + 1000 diluted) and an aliquot of it (10 mL) was mineralized with ultrapure H_2O_2 (1 + 1000 diluted) by MW digestion. A two-step MW digestion procedure, previously optimized [36], was applied with the following parameters: first ramp to 160 °C in 30 min, 1 min hold, second ramp to 170 °C in 30 min, 1 min hold, and finally, 15 min of cooling time. The filters containing the residue (insoluble fraction, Me$_{insol}$) from the water extraction were then totally solubilized and mineralized using the following two-step microwave digestion procedure, as previously optimized by Illuminati et al. [36]: first ramp to 135 °C in 36 min, 2 min hold, second ramp to 170 °C in 18 min, 4 min hold, and finally, 15 min of cooling time.

"Field blank" filters were subjected to the same treatments and the same MW digestion procedure as were applied to the sample filters.

To test the measurement additivity of the fractionation treatment with respect to the total content, another 1/8 of each original filter was directly MW digested using the same procedure as the insoluble fraction to obtain the total content. The results were then compared with the total content (Me_{tot}) computed from the sum of both the soluble and insoluble fractions.

2.4. Metal Determination

Metal determination in the MW-digested soluble and insoluble fractions was carried out by GF-AAS, except for the Pb and Cu soluble fractions, which were analyzed by anodic stripping voltammetry. Atomic absorption spectrometry standard solutions for Al, Fe, Cd, Pb, and Cu were used to build up the calibration curves. Hollow cathode lamps were used as a light source. Aluminum, iron, cadmium, lead, and copper were measured at wavelengths of 396.2, 248.3, 228.8, 283.3, and 327,4 nm, respectively. To improve the analytical measurements, for Cd, Pb, and Cu, a 0.2% Pd matrix modifier in citric acid was used. Further details of the instrumental parameters of the AAS applied for the metal determination are given in the Supplementary Material (Table S1).

The soluble concentrations of Pb and Cu were determined by square wave anodic stripping voltammetry (SWASV) in background subtraction mode, following a procedure set-up and optimized in our previous work [11,36]. An aliquot (10 mL) of the MW-digested solution was poured into a pre-cleaned voltammetric cell, where the thin mercury film electrode (TMFE) was already prepared and tested. The voltammetric analyses were carried out with the background subtraction technique using the following instrumental parameters: E_{dep} = −1100 mV; t_{dep} = 30 s for Cu and 10 min for Pb; E_{fin} = +120 mV; E_{equil} = −1100 mV; t_{equil} = 120 s; E_{precl} = −50 mV; t_{precl} = 5 min; E_{SW} = 20 mV; f = 150 Hz; ΔE_{step} = 8 mV; t_{step} = 100 ms. We performed 2–3 replicates with the sample in the cell, after which quantification was obtained using the multiple standard addition method.

2.5. Quality Control

The analytical quality control was performed by evaluating a series of blanks, accuracy, repeatability, and detection limits. The series of field blanks were analyzed with the same procedure as the environmental samples. As for the samples, the Pb and Cu soluble fractions of the field blanks were determined by SWASV.

Values due to blank filters are significant compared with the data of the exposed filters. In particular, blank values accounted for less than 10% for Al and Fe, 15–70% for Cd, 1–50% for Cu, and 30–55% for Pb, both in the two-fraction and total solutions. Similar values were obtained by our research group in previous studies on APM chemical fractionation [11,33,36] and by other authors when total MW digestions of sample filters were considered [10,40,41]. Moreover, blank values of up to 20% of the measured metal contents were reported for the certified reference material NIST SRM 1648, which contained a metal concentration much higher than ours [42]. Nevertheless, acceptable results of both accuracy and repeatability (see below) were obtained for the sample concentrations since field blanks to be subtracted showed repeatabilities of ≤10%, as a relative standard deviation. The metal concentrations determined in the five field blanks are reported as the mean ± SD in Table S2 of the Supplementary Material. The obtained values for the field blanks were subtracted from all the analytical measurements.

The detection limit (LOD) and the quantification limit (LOQ) were calculated for each metal using the following equations, according to ICH Q2B [43]:

$$LOD = 3.3 \, \frac{S_a}{b} \text{ and } LOQ = 10 \, \frac{S_a}{b}$$

where S_a is the standard deviation of the intercept of the regression line and b is the slope of the calibration curve. The LODs and LOQs obtained for each metal fraction are presented in Table 1.

Table 1. Limits of detection (LOD) and of quantification (LOQ) for the studied metals in the two fractions (soluble and insoluble) and in the direct measurement of total concentrations.

Metals	LODs in Solution [a] ($\mu g\ L^{-1}$)		LODs in Air [b] ($pg\ m^{-3}$)		LOQ in Solution [a] ($\mu g\ L^{-1}$)		LOQ in Air [b] ($pg\ m^{-3}$)	
	Soluble	Insoluble/Total	Soluble	Insoluble/Total	Soluble	Insoluble/Total	Soluble	Insoluble/Total
Al	1.2	4.7	28	101	3.7	14	86	958
Fe	2.2	8.1	24	187	3.2	24	73	567
Cd	0.01	0.004	0.28	0.08	0.04	0.01	0.83	0.25
Cu	0.11	0.09	2.3	2.2	1.4	0.28	4.2	6.5
Pb	0.02	0.12	0.38	2.8	0.04	0.15	0.92	3.5

[a] LOD for sample metal concentration in extraction solutions; [b] LOD for atmospheric metal concentration, calculated using the mean air volume of 17,216 m^3.

Furthermore, to assess the accuracy of the measurements carried out by GF AAS and SWASV, the certified reference material NIST 1648a for metals in urban particulate was analyzed. The NIST 1648a was treated with the same procedure used for the collected samples. The systematic measurements carried out on the reference material (n = 5–7) resulted in mean values ($\pm$SD) of Al 3.34 ($\pm$0.75)%, Fe 3.79 ($\pm$0.22)%, Cd 71.2 $\pm$8.0) mg kg^{-1}; Pb 0.623 ($\pm$0.067)%; Cu 590 ($\pm$38) mg kg^{-1}, against certified mean values ($\pm$95% confidence interval) of NIST 1648a: Al 3.43 ($\pm$0.13)%; Fe 3.92 ($\pm$0.21)%; Cd 73.7 ($\pm$2.3) mg kg^{-1}; Pb 0.655 ($\pm$0.033)%; Cu 610 ($\pm$70) mg kg^{-1}. The results are in good agreement with the certified reference values within the experimental errors, showing good accuracy for all the measurements.

The repeated determinations of Al, Fe, Cd, Pb, and Cu in the different PM_{10} samples resulted in an average repeatability (expressed as RSD%) of 6%.

2.6. Enrichment Factors

Enrichment factor (EF) calculation is a first step in the source apportionment evaluation to differentiate the possible sources of elements in the PM. In the present study, crustal enrichment factors were calculated for each metal according to the following equation:

$$\mathrm{EF_i} = \frac{(C_i/C_r)_{air}}{(C_i/C_r)_{source}}$$

where $\mathrm{EF_i}$ is the EF of the element i, r is the reference element, $(C_i/C_r)_{air}$ is the concentration ratio of the element i over the reference element r in the aerosol, and $(C_i/C_r)_{source}$ is the abundance ratio of the element i over the reference element r in the source materials.

Generally, Al is the reference element for a crustal source and it has been widely used to calculate crustal enrichment factors (CEFs) in the Southern Ocean and Antarctica [6,10–12]. The average upper continental crust (UCC) composition reported by Wedepohl [44] was used here to facilitate the comparison with other studies. The CEF was calculated for each metal according to the following equation:

$$\mathrm{EF_i} = \frac{(C_i/C_{Al})_{PM}}{(C_i/C_{Al})_{UCC}}$$

where $(C_i/C_{Al})_{PM}$ is the concentration ratio of the element i over the reference element Al in the atmospheric particulate matter, and $(C_i/C_{Al})_{UCC}$ is the abundance ratio of the element i over the reference element Al in the upper continental crust.

Values of CEFs near unity suggest crustal weathering as predominant sources of the element i. According to Tuncel et al. [45], values less than unity indicate depletion with respect to the source materials or a poor choice of the normalizing element. Values greater than unity indicate possible additional sources or chemical fractionation upon entering the atmosphere. Most crustal elements are characterized by 1 < EFs < 5, but these elements are not considered enriched since differences in crust composition from various areas must be taken into account. Therefore, EFs < 10 indicate the element has a prevailing geogenic or

marine origin, 10 < EF < 100 indicated the element was moderately enriched, and EF > 100 indicated the element was greatly enriched.

2.7. Air Mass Back Trajectories

In order to define the origin of the air masses arriving at MZS, 120 h backward trajectories every three hours were calculated using the Hybrid Single-Particle Lagrangian Integrated Trajectories (HYSPLIT) model developed by NOAA and Australia's Bureau of Meteorology [46]. The back trajectories were computed for four heights (500 m, 1000 m, 1500 m, and 2000 m above the ground level, a.g.l.) at the MZS, for the period spanning 1 December 2013 to 2 February 2014, corresponding with the aerosol sampling collection period. The meteorological data used for computing the backwards trajectories (TJs) were the National Weather Service's National Centers for Environmental Prediction (NCEP) global data assimilation system (GDAS) model data, with a regular grid of $0.5° \times 0.5°$ [47]. In accordance with Mezgec et al. [48] and Caiazzo et al. [49], the whole domain was divided into a cell grid of 4° (lat) $\times$ 1° (long), and the number of TJs passing from each cell was calculated. Counting of the TJs was performed for the whole trajectory period (see more details in Section 3.3) as well as separately for the months of December and January, with the aim of highlighting the monthly variability. A filter was applied to count only the TJs that spent at least 20% of the time (1 day) at heights between 100 and 1000 m, in order to consider the only TJs able to load and transport aerosols. The 20% threshold is arbitrary; however, changing it to ±10% did not lead to substantial differences. The choice of 5 days was made assuming the expected lifetime for aerosols in this region (usually less than a week, depending on aerosol properties and meteorological conditions) [1,5].

3. Results and Discussion

3.1. Total Metal Concentrations in the Atmosphere over Terra Nova Bay

The total concentrations of the elements in the PM_{10} at Faraglione Camp (Antarctic summer 2013–2014) are shown in Table 2 and Table S3. The results are reported as the sum of the two fractions obtained in the sequential extraction procedure and as direct measurements of the total concentrations. Atmospheric concentrations refer to both actual (mean temperature, 270 K and mean pressure, 970 hPa) and to standard air (298 K, 1013 hPa).

First, it can be noted that the metal concentrations referring to the actual air are similar to those referring to the standard air; in fact, differences are below 1%. Thus, the correction computed for standard air is negligible if compared with the precision in the volume sampled (±10%). By consequence, in the following paragraphs, results referring to actual air will be discussed.

Table 2 and Table S3 show, moreover, that the sum of the soluble and insoluble metal fractions from any 10-day sampling period was in good agreement with the total measured PM_{10} metal concentrations, with differences between the two values ranging from −10% and +30%. The only exception was represented by Cd, relatively to the third (collected from 22 December 2013 to 3 January 2014) and to the sixth (collected from 23 January 2014 to 2 February 2014) samples (Table 2), where differences between the sum of the metal fractions and the total measured content in the PM_{10} exceeded ~50%. This discrepancy is due to possible contamination of the two samples. Therefore, these values will be excluded in the following discussion and will be substituted by the corresponding values obtained through the indirect measurement. The additivity test performed here and the resulting agreement suggest that the sequential extraction procedure and the analyses were performed quantitatively.

Table 2. Atmospheric concentrations of the studied metals (Al, Fe, Cd, Cu, and Pb) as the sum of different metal fractions (soluble + insoluble fractions) and as direct measurements at Faraglione Camp during the austral summer 2013–2014. Concentrations refer to actual air.

Sampling Period	Actual Air Volume (m³)	Atmospheric Concentration [a]				
		Al (ng m⁻³)	Fe (ng m⁻³)	Cd (pg m⁻³)	Cu (pg m⁻³)	Pb (pg m⁻³)
Computed total PM10 from chemical fractionation						
01/12/13–12/12/13	18,400	26 ± 2	27 ± 2	0.69 ± 0.12	30 ± 4	9.5 ± 1.3
12/12/13–22/12/13	16,311	20 ± 2	20 ± 2	1.1 ± 0.2	41 ± 4	21 ± 3
22/12/13–03/01/14	19,578	22 ± 2	25 ± 2	1.9 ± 0.3	56 ± 5	15 ± 2
03/01/14–13/01/14	16,397	29 ± 2	21 ± 2	0.55 ± 0.12	55 ± 6	22 ± 3
13/01/14–23/01/14	16,341	24 ± 2	28 ± 2	0.82 ± 0.27	38 ± 5	15 ± 2
23/01/14–02/02/14	16,271	25 ± 2	16 ± 1	3.1 ± 0.3 *	41 ± 4	10 ± 1
Total measured PM10						
01/12/13–12/12/13	18,400	19 ± 2	21 ± 2	0.74 ± 0.10	28 ± 3	11 ± 2
12/12/13–22/12/13	16,311	19 ± 2	21 ± 2	1.0 ± 0.2	48 ± 8	21 ± 3
22/12/13–03/01/14	19,578	23 ± 2	24 ± 3	4.9 ± 0.9 *	57 ± 7	14 ± 2
03/01/14–13/01/14	16,397	27 ± 3	24 ± 3	0.48 ± 0.09	47 ± 6	22 ± 3
13/01/14–23/01/14	16,341	25 ± 3	24 ± 3	0.69 ± 0.10	28 ± 4	15 ± 2
23/01/14–02/02/14	16,271	19 ± 2	18 ± 2	0.70 ± 0.12	40 ± 6	10 ± 2

[a] $\pm$ SD computed as the square root of the sum of variances. * anomalous values.

The total metal concentrations measured in the PM_{10} at Faraglione Camp during austral summer showed the following values, given as means (min–max range): Al, 22 (19–27) ng m⁻³; Fe, 22 (18–25) ng m⁻³; Cd, 1.4 (0.39–2.0) pg m⁻³; Cu, 40 (28–57) pg m⁻³; Pb, 16 (10–22) pg m⁻³. Therefore, the following decreasing trend over Terra Nova Bay can be observed: Al $\approx$ Fe > Cu > Pb > Cd.

The total metal concentrations obtained in this study were compared to the literature data available from the same and/or other Antarctic areas and from several regions worldwide (Table 3). Our Al and Fe values are higher (2–3 times) than those recorded in previous surveys at Faraglione Camp [10,13]. These aerosol Al and Fe concentrations were also higher than the 10-year values of the total suspended particles (TSP) measured at the South Pole [6–8,45], but they were comparable to the 4-year values of 9.9 and ~13 ng m⁻³, respectively, at King Georg Island [50,51]. Al atmospheric content, moreover, was higher than the summer mean of 4.3 ng m⁻³ recorded on Anvers Island [52] and it was lower than the concentrations recorded in the Southern Ocean [12]. Fe_{tot} fell within the ranges over the Southern Ocean (from 6 to 38 ng m⁻³) and in coastal East Antarctica (14–56 ng m⁻³) [12,53]. The total atmospheric concentrations of trace metals (Cd, Cu, and Pb) are in good agreement with those previously reported for the same study site, with the only exception of Cu [10,11,13,33], for which values 1 order of magnitude higher were recorded by Toscano et al. [10] and Annibaldi et al. [11]. A general agreement with our Cd, Cu, and Pb values was observed in studies carried out in other Antarctic areas [4,52,54].

However, all the metal values were much lower than the average metal concentrations recorded at two sites of McMurdo Station [9], probably due to the impact of the McMurdo Dry Valleys in this part of Antarctica. In fact, several studies reported McMurdo Sound as the dustiest site in Antarctica (Winton et al., [55] and references therein).

The comparison with the literature data referring to anthropized areas showed Al and Fe contents 1–2 orders of magnitude lower than other areas worldwide, Cd_{tot} 3–4 orders of magnitude lower than those recorded in anthropized areas, and Pb and Cu concentrations 3–5 orders of magnitude lower even than background areas (Table 3).

Table 3. Summary of atmospheric metal (Al, Fe, Cd, Cu, and Pb) concentrations measured in various Antarctic locations and in other areas worldwide.

Site	Sampling Period	PM Fraction	Atmospheric Metal Concentrations					References Data
			Al, ng m^{-3}	Fe, ng m^{-3}	Cd, pg m^{-3}	Cu, pg m^{-3}	Pb, pg m^{-3}	
Terra Nova Bay	Summer 2013–2014	PM$_{10}$	24 ± 3	23 ± 5	1.0 ± 0.5	44 ± 10	15 ± 5	This work
	Summer 2010–2011	PM$_{10}$	5.08	3.54	–	32.5	22.5	[13]
	Summer 2001–2002	PM$_{10}$	2.84–13.5	2.74–10.99	–	121–1102	6.8–48.7	[10]
	Summer 2000–2001 *	PM$_{10}$	–	–	3.4 ± 2.2	266 ± 103	24 ± 171	[11]
	Summer 2000–2001	PM$_{10}$	–	–	9.5 ± 13.1	340 ± 150	33 ± 16	[33]
McMurdo Hut Point	Summers 1995–1997	PM$_{10}$	183 ± 40	131 ± 34	–	189 ± 5	828 ± 428	[9]
Radar Sat	Summers 1995–1997	PM$_{10}$	251 ± 43	163 ± 23	–	198 ± 45	460 ± 160	[9]
East Antarctica	Nov 2010–Mar 2011	PM$_{10}$	190	27	17	–	–	[12]
Dome C	Dec 2005–Jan 2006	PM$_{10}$	–	–	0.24 ± 0.13	120 ± 70	21 ± 8	[54]
	Summer1970–1971	TSP	0.57 ± 0.17	0.84 ± 0.21	–	36 ± 9	630 ± 300	[6]
	Summer1974–1975	TSP	0.82 ± 0.38	0.62 ± 0.23	≤18	29 ± 17	76 ± 40	[7]
South Pole Amundsen-Scott St	Summer1971–1978	TSP	0.83 ± 0.25	0.68 ± 0.25	49 ± 38	59 ± 47	–	[8]
	Winter1975–1976	TSP	≤0.30	0.25 ± 0.12	<200	79 ± 16	–	[8]
	Summer1979–1983	TSP	0.73 ± 0.24	0.66 ± 0.28	110 ± 60	190 ± 130	–	[45]
	Winter1979–1983	TSP	0.32 ± 0.11	0.28 ± 0.12	50 ± 40	130 ± 80	–	[45]
Larsen Ice ShelfGipps Ice Rice	Summer 1984–1985	TSP	194 ± 19	–	0.06 ± 0.1	1.0 ± 1.0	4.7 ± 0.8	[56]
Ekström Ice Shelf, Neumayer St.	Mar 1999–Dec 2003		1.0 ± 0.7	–	–	–	–	[16]
	Feb 1983–Dec 1984	TSP	–	–	–	–	11 ± 1.5	[57]
Anvers Isl.	Nov 2016–Jan 2017	PM$_{10}$	4.3 ± 2.4	–	–	150 ± 150	19 ± 19	[52]
Deception Isl.	Dec 2016–Feb 2017	PM$_{10}$	–	–	–	0.6–2100	40–490	[4]
King Georg Island								
Comandante Ferraz Station	Summer/Winter	<2 µm	3.37 ± 2.81	1.25 ± 1.80	–	130 ± 90	170 ± 110	[50,51]
	1985–1988	2.0–15.0 µm	9.94 ± 8.07	12.9 ± 13.4	–	620 ± 570	630 ± 590	
King Sejong	Jan 2000–Dec 2001	TSP	1875 ± 3285	–	1.3 ± 3	143 ± 471	41 ± 54.5	[58]
Southern Ocean	Nov 2010–Mar 2011	PM$_{10}$	150	14	4	–	–	[12]
Europe	2001	PM$_{10}$	2069	628	264	19,033	17,040	[59,60]
China		PM$_{10}$	–	–	13,000	217,000	261,000	[61]
South Brazil	Nov 2001–Nov 2002	PM$_{10-2.5}$	594	15.3	–	–	6700	[62]
Argentina	May 2014–Nov 2016	PM$_{2.5}$	208.8	156.8	12,000	7100	8600	[63]
Chile	1997–2003	PM$_{10}$	3030	–	3571	175,000	394,000	[64]
Australia	1993–1995	PM$_{10}$	587	450	–	–	104,000	[65]
South Africa	Nov 2010–Dec 2011	PM$_{10}$	170	1200	400	6900	7800	[66]

* Concentrations referred to the total HCl-extractable metal fraction.

The total atmospheric concentration of Cd ranged from 0.5 to 1.9 pg m^{-3}, with a maximum (1.9 ± 0.3 pg m^{-3}) at the end of December. A similar summer evolution was observed for Cu and Pb, with maximum values of ~50 pg m^{-3} and ~21 pg m^{-3}, respectively. While the maximum for Cu$_{tot}$ occurred at the end of December, as it did for Cd, Pb$_{tot}$ immediately increased at the beginning of the month and maintained these values until the end of January. The seasonal evolution of Cd, Cu, and Pb was already observed at Faraglione Camp during previous surveys [11,13,33]. Studies on the seasonal evolution of trace metals in Antarctica have been very sporadic. Summer trends of trace metals similar to ours were observed by Dick et al. [56] studying the inorganic chemical composition of TSP over the Antarctic Peninsula during the austral summer of 1984/1985. Al$_{tot}$ and Fe$_{tot}$ showed a discrete variability from one sampling to another. However, the overall evolution of these two metals was quite constant during the field campaign, with summer means of ~24 ng m^{-3} and ~23 ng m^{-3}, respectively. The few datasets available indicated a fairly uniform variation of Al and Fe concentration over Antarctica during summer [10,13].

3.2. Metal Partitioning in the Antarctic Aerosol

Chemical fractionation results obtained for the PM$_{10}$-bound metals at Faraglione Camp are shown in Figure 3. A different fractionation pattern can be recognized in each studied metal.
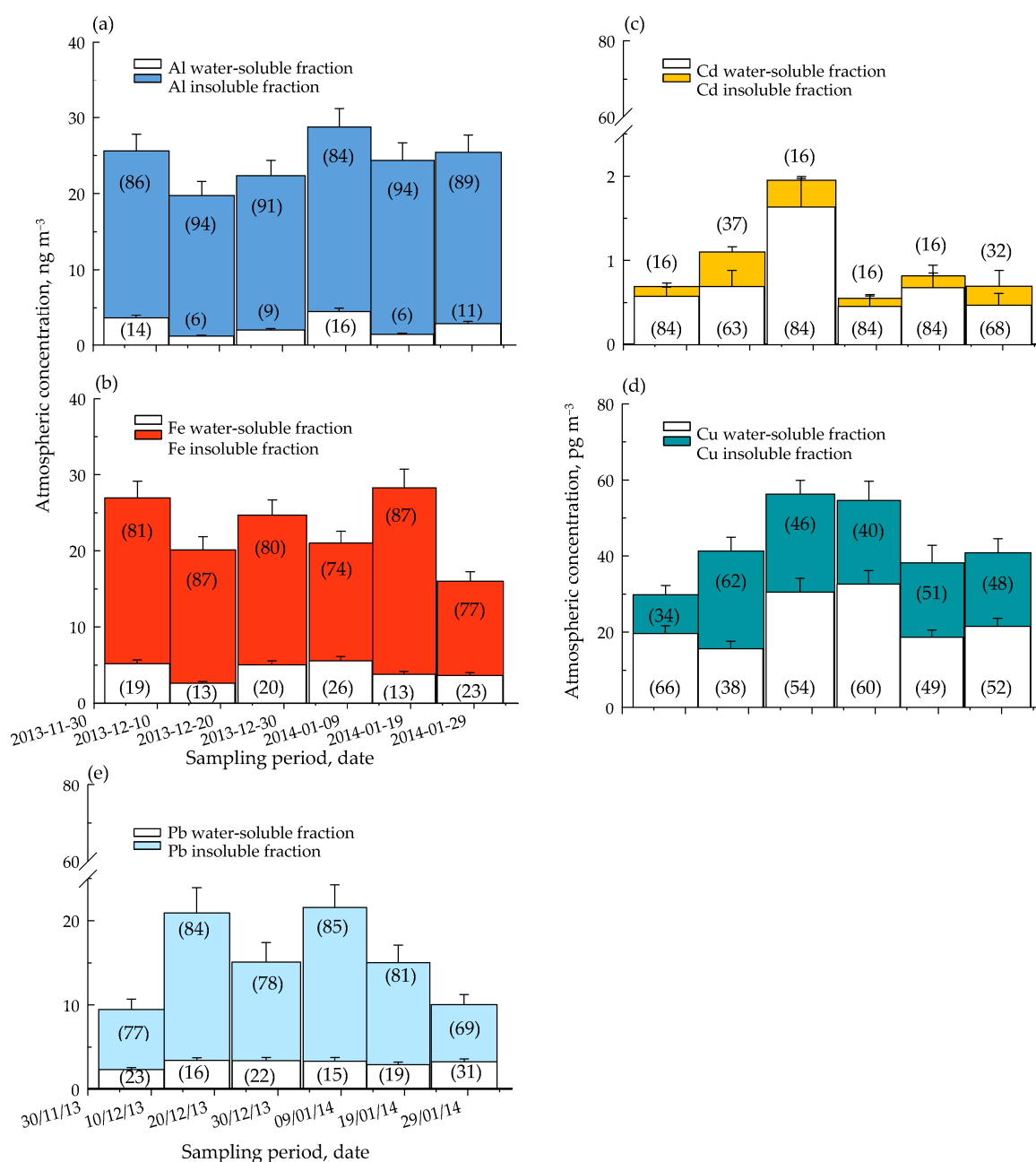
Figure 3. Seasonal evolution of Al (**a**), Fe (**b**), Cd (**c**), Cu (**d**), and Pb (**e**) partitioning between water-soluble and residual fractions in the PM_{10} collected at Terra Nova Bay (Ross Sea, Antarctica). In brackets, fraction percentages with respect to the total PM_{10}-bound metal concentration.

Distributions of Al and Fe were very similar. As expected, these two PM_{10} minor constituents appeared mostly in the insoluble fraction, accounting for 90–95% of the total atmospheric concentration in the PM_{10} (Figure 3a,b). The insoluble fractions remained almost constant during summer, with values ranging from 17 ng m^{-3} to 24 ng m^{-3} for Al (Figure 3a) and from 12 ng m^{-3} to 24 ng m^{-3} for Fe (Figure 3b). The percentages of Al_{sol} and Fe_{sol} with respect to the total were relatively low (~5–20%), showing very little variation during the sampling period (Figure 3).

The trace element Cd was mostly present in the water-soluble fraction. This fraction varied from ~0.5 to 1.6 pg m^{-3} and accounted for 60–80% of the total Cd concentration in the PM_{10} (Figure 3c). Both soluble and insoluble fractions of Cd showed a bell-shaped evolution during summer, with maximum values at the end of December (Figure 3c).

However, their contribution to the total remained almost constant (Cd_{sol} ~20% and Cd_{insol} ~80% of the total).

Among the trace metals studied, Pb insoluble fraction showed the highest proportion, with a mean percentage of ~80% of the total concentration (Figure 3e). Pb_{insol} varied from ~7.0 pg m^{-3} to ~18 pg m^{-3} during the summer, with high values from mid-December to the beginning of January. The Pb soluble fraction remained almost constant during the season (mean $\pm$ SD, 3.0 ± 0.4 pg m^{-3}), accounting for ~20% of the Pb_{tot} (Figure 3e).

Cu in the PM_{10} was almost equally distributed between soluble and insoluble fractions, with percentages varying from ~30% to ~65% of the total concentration during summer (Figure 3d). Both fractions showed a bell-shaped variation with a shift in the maximum occurrence during summer. Cu_{insol} varied from 10 to 26 pg m^{-3} with maximum values at mid-December, while the Cu_{sol} peak (33 pg m^{-3}) occurred in mid-January (Figure 3d).

Very few studies on the chemical fractionation of metals in the APM have been carried out in Antarctica. Trace metal partitioning patterns presented here are in good agreement with our previous surveys at Faraglione Camp [11,33]. During the austral summers 2000–2001 and 2001–2002, Annibaldi et al. [11] and Truzzi et al., [33] carried out a three-step SEP, thus distinguishing the water-soluble, HCl-extractable, and inert fractions of Cd, Pb, and Cu. The authors observed a prevalence of the insoluble metal fractions at the beginning of summer due to both anthropogenic activities and crustal dust transported by catabatic winds. When the pack ice melted, the soluble metal fractions prevailed. In our work, only Cu showed a behavior as previously described, while Cd and Pb fractions showed a different seasonal evolution, with Cd_{sol} and Pb_{insol} prevailing for the entire sampling period (Figure 3).

Concerning Al and Fe fractionation, no data are available for the polar regions. However, their soluble–insoluble partitioning was similar to other surveys carried out worldwide [22,30,67]. Different extracting solutions and different extraction procedures are currently used to separate the soluble fraction from the solid residue [31]. The simple treatment with ultrapure water or the ultrasonication in ultrapure water are the most used methods to determine the Me_{sol} in APM. Our percentages of Al_{sol} and Fe_{sol} (varying from 10% to 20%), with respect to the total concentrations, were in agreement with those reported by Jiang et al. [67] (in the $PM_{2.5}$, Al < 20% and Fe from 20% to 60%; in the coarse PM, Al and Fe <10%), who also recorded a significant size-dependent trend for certain elements by applying only ultrapure water to extract the soluble metal fractions.

Water-soluble proportions of Fe were found $\leq$10% in the PM_{10} collected in Edinburgh by Heal et al. [30]. Similar percentages of Fe_{sol} were recorded by Li et al. [22] in urban sites of China. Our Al_{sol} and Fe_{sol} percentages were also similar to those recorded by other surveys where the ultrasonication technique in ultrapure water was applied [20,23,68]. It is worth noting that this procedure gives percentages of extraction slightly higher (15–20%) than those obtained by the extraction procedure with only the ultrapure water [31].

Our results for Al_{sol} and Fe_{sol} were higher than the values found in Saharan dust or in other arid continental soils (up to 2–5% [69,70]), comparable with those recorded over the Southern Ocean and in remote areas of the Atlantic Ocean (7.6–26% for Al_{sol} and 4.0–19% for Fe_{sol} [53,70]) and lower than values recorded for the North Atlantic/Europe region (13–86% for Al_{sol} and 15–54% for Fe_{sol} [70,71]). When comparing data on aerosol metal solubilities vs. total airborne metal content derived from studies carried out worldwide, it has to be noted that there are significant differences in the collection methods and in the extraction procedures. However, Sholkovitz et al. [69], in their extensive compilation of aerosol iron solubility estimates for samples collected around the globe, noted a systematic trend over regional and global scales that seemed to dominate any effects related to methodological differences. Our data are also consistent with the overall estimation of the Fe soluble fraction as obtained by the global oceanic biogeochemical budgeting calculations [69,70]. Moreover, the Fe_{sol}/Fe_{tot} proportion agreed with the study by Sholkovitz et al. [69] reporting that the fractional solubility of aerosol Fe (defined as $Fe_{sol}/Fe_{tot} \times 100$) entering the ocean can be significantly higher than the value of ~1% that is typical of the continental

soils. A number of factors influence aerosol Fe solubility estimates, for example, atmospheric dust concentration, particle size, wet and dry depositions, chemical–photochemical atmospheric processes, and aerosol sources [53,69,70]. The debate over what the effective solubility of aerosol Fe is and how this solubility is related to the fraction of deposited Fe that is available for phytoplankton growth is still ongoing [71,72].

3.3. Source Identification

The main sources of atmospheric particulate material in Antarctica are wind-blown crust dust and the ocean. To gain more information on the possible sources of metals in the aerosol over Terra Nova Bay, the EFs for Fe, Cd, Cu, and Pb were calculated. Figure 4 shows the box-and-whisker plots of crustal and sea salt enrichment factors. It can be noted that Fe and Pb had the lowest CEFs (with the median value lower than 3), with enrichment factor values decreasing in the following order: Cd > Cu > Pb $\approx$ Fe.
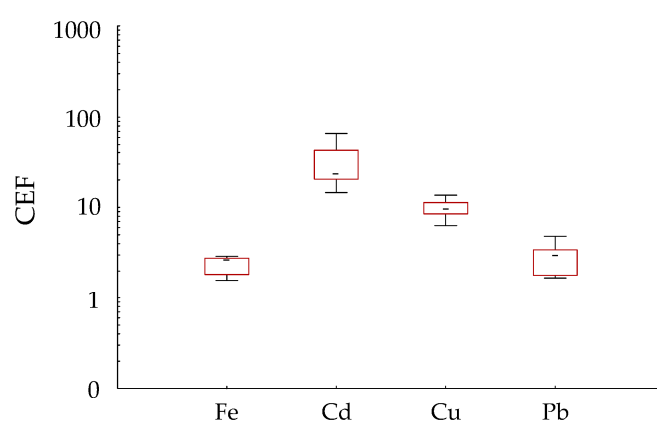
Figure 4. Box-and-whisker plots of CEFs (values reported in logarithmic scale) for metals in the PM_{10} collected at Faraglione Camp (Terra Nova Bay, Antarctica) between December 2013 and February 2014. The central horizontal line is the median value, and the bottom and the top of each box are the 25th and 75th percentiles. The upper and lower horizontal bars indicate the 5th and 95th percentiles of the data.

According to the results, Fe may be attributable to crustal local inputs, confirming the results of previous studies carried out in the same study area [10,13,14] and in other Antarctic regions [73,74].

The median values of CEF for Cd were higher than 10, suggesting possible contributions from non-crustal sources for this metal. The Cd EF is in good agreement with our previous surveys and with other studies on metals in Antarctic aerosol [11–13,33] and surface snow [75,76]. Sea salt spray, marine biogenic activity [77], volcanic emission, and anthropogenic inputs [13,75,76,78] could be considered additional sources to explain the enrichment of Cd in the PM_{10} over Terra Nova Bay. In accordance with Planchon et al. [78], we estimated the sea spray contribution to the PM_{10} from the Na concentration in the aerosol, as measured by Bazzano et al. [13], and the mean seawater concentrations in the Antarctic surface waters, as reported by Illuminati et al. [79] and Corami et al. [80]. In order to take into account the influence of marine aerosols formed by bubbles bursting through the sea surface microlayer to the PM_{10}-bound metals, we applied enrichment factors of 1000 for Fe, 200 for Cd and Cu, and 100 for Pb, as reported by Annibaldi et al. 2007 [11] and Planchon et al. [78] (and references therein). Therefore, the following sea-spray contributions were estimated: Cd—25%, Cu—2%, Pb—0.8%, and Fe—0.01%.

The study site and MZS are close to the quiescent volcano, Mount Melbourne, for which a moderate fumarolic activity in the summit area was well documented [81]. To assess the possible volcanic contribution, the sulfate concentration in the PM_{10} collected at the same site by Barbaro et al. [14] was combined with the estimated metal/S ratios in Mount Erebus (an active volcano ~200 km far from MZS) emissions [82] by assuming that

∼13% of non-sea-salt sulfate originates from volcanoes [83]. This source contributed <1% to the content of each metal in the PM_{10}.

The marine biogenic activities can also contribute to the metal content in PM_{10}. It is known that some metals (Pb, Cd, Hg) can be methylated in the ocean by polar marine microorganisms (bacteria, microalgae) [77]. These organometal compounds can be emitted into the atmosphere and, therefore, contribute to the enrichment of some metals in the APM. However, the available data do not allow for any estimation of this possible contribution.

Our raw estimations confirmed anthropogenic activities as a potential source of Cd in the Antarctic PM_{10}, as reported in previous studies [11,75]. In addition to local inputs, we cannot exclude a long-range transport of Cd-contaminated PM_{10} from Southern America and Australia due to mining and smelting activities, as reported in previous surveys [4,13,14].

Surprisingly, Pb and Cu showed low CEFs, suggesting a crustal origin. These results are in contrast with the literature data, which suggest the possible local or long-range influence of anthropogenic processes on Antarctic regions [4,13,73]. In particular, although Pb concentrations have drastically decreased in snow and firn during the 1990s and 2000s, due to the phasing-out of leaded gasoline [84], the determination of lead isotope ratios by Bazzano et al. [13] at Faraglione Camp showed significant contributions (50–70% for Pb) of polluted aerosols from anthropized areas (e.g., South America, Australia).

A possible explanation of these unexpected results on Pb sources is the frequent katabatic wind events characterizing the 2013–2014 summer season and continuing until the beginning of January (Figure 2). This strong wind, blowing from the Antarctic plateau to coastal areas, could move any possible local contamination by Pb and Cu from the study site. However, Cu showed a low to moderate enrichment during the season, with values just above 10. Therefore, a possible enrichment from marine aerosol and/or from local anthropogenic input cannot be excluded for this metal.

Finally, it has to be pointed out that enrichment factors must be used with caution in the source apportionment analysis since they are only an approximation of the crustal aerosol composition [10].

Figure 5 shows the 5-day air mass backward trajectories calculated for four heights (500 m, 1000 m, 1500 m, and 2000 m a.g.l.) using the HYSPLIT model. The results of the TJ analysis confirmed that Terra Nova Bay was mainly affected by air masses originating from the Antarctic plateau and reaching the sampling site at very high speeds (Figure 5). A certain number of TJs arriving at MZS in December were derived in part from the Southern Ocean from the Australian sector. To investigate the long-range transport, an additional threshold was imposed considering only TJs between 100 m and 1000 m, as well as below 48 S for almost 6 h (i.e., 5% of the time). The results (not shown) show a short passage close to the Tasmanian coasts, suggesting a weak contribution from that area.

In January, the air mass scenario was mainly localized to the Antarctic continent. The contribution from the inland areas still prevailed, but air masses coming from the east or the southeast were also observed, suggesting an increase in the marine input on the study site (Figure 5c).

The air mass back trajectory analysis as well as the CEF calculations applied to our results were not exhaustive in establishing the possible sources of the metals studied. As for enrichment factors, the trajectory data had to be used with caution due to the number of uncertainties in the trajectory models [85].

Further data (higher temporal resolution of the sample collection, determination of many other metals and major ions, analysis of the source apportionment) are necessary to confirm the speculations, argumentations, and hypotheses formulated here for the interpretation of the results.
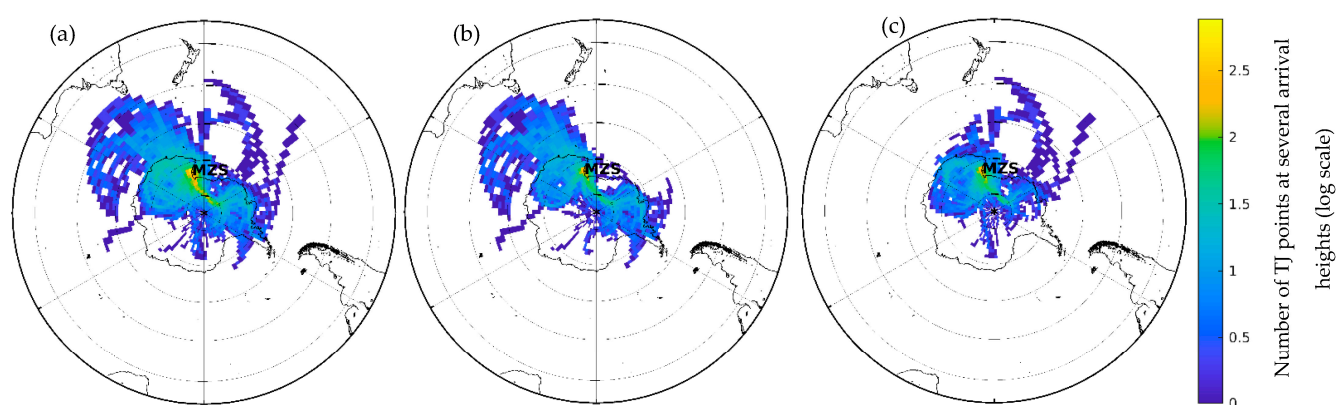
Figure 5. Total number of trajectories arriving at 500, 1000, 1500, and 2000 m above MZS, laying within each cell grid (4° × 1°). Panel (**a**) refers to the whole trajectory dataset, panel (**b**) to December, and panel (**c**) refers to January. Data are reported on a logarithmic scale.

4. Conclusions

This study presents the content of two minor constituents (Al and Fe) and three trace elements (Cd, Cu, and Pb) in PM_{10} samples collected at Terra Nova Bay during the austral summer of 2013–2014. Concentrations, metal partitioning, temporal variation, and sources were thoroughly discussed.

The metal fractionation obtained through a two-step extraction procedure showed that Al, Fe, and Pb were mainly present in the insoluble fraction, accounting for 80% to 95% of the total element concentration. On the contrary, Cd appeared to be the most mobile metal since its soluble fraction (60–80% of the total concentration) prevailed on the residual fraction for the entire summer season. Finally, Cu was almost equally distributed between soluble and insoluble fractions, with percentages varying from ~30% to ~65% of the total concentration.

Al and Fe showed an overall constant trend of both fractions during the summer season, while a bell-shaped evolution was observed for the three trace metals. Cd and Cu maximum concentrations occurred in mid-December when the pack ice melted and involved both fractions. The Pb insoluble fraction immediately increased at the beginning of summer, then maintained these values until the end of January, while the soluble fraction remained almost constant.

Taking crustal EFs into account, we hypothesized that Cd was mainly influenced by a marine source, especially when the pack ice melted and, possibly, by anthropogenic inputs of local origin and/or for long-range transport. To a lesser extent, additional marine and/or anthropogenic sources could also influence the concentration of Cu in the PM_{10}.

Al and Fe were mainly related to crustal inputs. Surprisingly, Pb also appeared to have a natural source, probably due to the frequent and strong katabatic wind events that characterized the 2013–2014 summer season, moving any possible local contamination by the metal.

The five-day air back trajectories showed a strong contribution of air masses derived from the Antarctic plateau during the entire sampling period, even if a potential contribution of the long-range transport from anthropized areas cannot be excluded. In January, the marine input from the Ross Sea ice-free areas started to be more significant.

Our results mark the importance of the continuous monitoring of the atmospheric particulate matter in polar regions. However, we recognize that further studies are necessary to gain a deeper understanding of the sources of metals in the Antarctic aerosol, the role of meteorological parameters, and the contribution of long-range transport. A more complete scenario could be obtained by determining many other trace metals and major ions and by analyzing the size-resolved chemical composition of PM_{10}, for which few studies are available for Antarctic areas.

References

1. Prospero, J.M.; Charlson, R.J.; Mohnen, V.; Jaenicke, R.; Delany, A.C.; Moyers, J.; Zoller, W.; Rahn, K. The atmospheric aerosol system: An overview. *Rev. Geophys.* **1983**, *21*, 1607–1629. [CrossRef]
2. Seinfeld, J.H.; Pandis, S.N.; Noone, K. Atmospheric Chemistry and Physics: From Air Pollution to Climate Change. *Phys. Today* **1998**, *51*, 88–90. [CrossRef]
3. Bargagli, R. Atmospheric chemistry of mercury in Antarctica and the role of cryptogams to assess deposition patterns in coastal ice-free areas. *Chemosphere* **2016**, *163*, 202–208. [CrossRef]
4. Marina-Montes, C.; Pérez-Arribas, L.V.; Escudero, M.; Anzano, J.; Cáceres, J.O. Heavy metal transport and evolution of atmospheric aerosols in the Antarctic region. *Sci. Total Environ.* **2020**, *721*, 137702. [CrossRef]
5. Budhavant, K.; Safai, P.D.; Rao, P.S.P. Sources and elemental composition of summer aerosols in the Larsemann Hills (Antarctica). *Environ. Sci. Pollut. Res.* **2015**, *22*, 2041–2050. [CrossRef]
6. Zoller, W.H.; Gladney, E.S.; Duce, R.A. Atmospheric concentrations and sources of trace metals at the South Pole. *Science* **1974**, *183*, 198–201. [CrossRef]
7. Maenhaut, W.; Zoller, W.; Duce, R.; Hoffman, G. Concentration and size distribution of particulate trace elements in the south polar atmosphere. *J. Geophys. Res.* **1979**, *84*, 2421–2431. [CrossRef]
8. Cunningham, W.C.; Zoller, W.H. The chemical composition of remote area aerosols. *J. Aerosol Sci.* **1981**, *12*, 367–384. [CrossRef]
9. Mazzera, D.M.; Lowenthal, D.H.; Chow, J.C.; Watson, J.G.; Grubĭsíc, V. PM10 measurements at McMurdo Station, Antarctica. *Atmos. Environ.* **2001**, *35*, 1891–1902. [CrossRef]
10. Toscano, G.; Gambaro, A.; Moret, I.; Capodaglio, G.; Turetta, C.; Cescon, P. Trace metals in aerosol at Terra Nova Bay, Antarctica. *J. Environ. Monit.* **2005**, *7*, 1275–1280. [CrossRef] [PubMed]
11. Annibaldi, A.; Truzzi, C.; Illuminati, S.; Bassotti, E.; Scarponi, G. Determination of water-soluble and insoluble (dilute-HCl-extractable) fractions of Cd, Pb and Cu in Antarctic aerosol by square wave anodic stripping voltammetry: Distribution and summer seasonal evolution at Terra Nova Bay (Victoria Land). *Anal. Bioanal. Chem.* **2007**, *387*, 977–998. [CrossRef]
12. Xu, G.; Gao, Y. Atmospheric trace elements in aerosols observed over the Southern Ocean and coastal East Antarctica. *Polar Res.* **2014**, *33*, 23973. [CrossRef]
13. Bazzano, A.; Soggia, F.; Grotti, M. Source identification of atmospheric particle-bound metals at Terra Nova Bay, Antarctica. *Environ. Chem.* **2015**, *12*, 245–252. [CrossRef]
14. Barbaro, E.; Zangrando, R.; Kirchgeorg, T.; Bazzano, A.; Illuminati, S.; Annibaldi, A.; Rella, S.; Truzzi, C.; Grotti, M.; Ceccarini, A.; et al. An integrated study of the chemical composition of Antarctic aerosol to investigate natural and anthropogenic sources. *Environ. Chem.* **2016**, *13*, 867–876. [CrossRef]
15. Wolff, E.W.; Barbante, C.; Becagli, S.; Bigler, M.; Boutron, C.F.; Castellano, E.; de Angelis, M.; Federer, U.; Fischer, H.; Fundel, F.; et al. Changes in environment over the last 800,000 years from chemical analysis of the EPICA Dome C ice core. *Quat. Sci. Rev.* **2010**, *29*, 285–295. [CrossRef]
16. Weller, R.; Wöltjen, J.; Piel, C.; Resenberg, R.; Wagenbach, D.; König-Langlo, G.; Kriews, M. Seasonal variability of crustal and marine trace elements in the aerosol at Neumayer station, Antarctica. *Tellus B Chem. Phys. Meteorol.* **2008**, *60 B*, 742–752. [CrossRef]

17. Becagli, S.; Scarchilli, C.; Traversi, R.; Dayan, U.; Severi, M.; Frosini, D.; Vitale, V.; Mazzola, M.; Lupi, A.; Nava, S.; et al. Study of present-day sources and transport processes affecting oxidised sulphur compounds in atmospheric aerosols at Dome C (Antarctica) from year-round sampling campaigns. *Atmos. Environ.* **2012**, *52*, 98–108. [CrossRef]

18. Feng, X.D.; Dang, Z.; Huang, W.L.; Yang, C. Chemical speciation of fine particle bound trace metals. *Int. J. Environ. Sci. Technol.* **2009**, *6*, 337–346. [CrossRef]

19. Illuminati, S.; Annibaldi, A.; Truzzi, C.; Tercier-Waeber, M.-L.; Nöel, S.; Braungardt, C.B.; Achterberg, E.P.; Howell, K.A.; Turner, D.; Marini, M.; et al. In-situ trace metal (Cd, Pb, Cu) speciation along the Po River plume (Northern Adriatic Sea) using submersible systems. *Mar. Chem.* **2019**, *212*, 47–63. [CrossRef]

20. Dos Santos, M.; Gómez, D.; Dawidowski, L.; Gautier, E.; Smichowski, P. Determination of water-soluble and insoluble compounds in size classified airborne particulate matter. *Microchem. J.* **2009**, *91*, 133–139. [CrossRef]

21. Smichowski, P.; Polla, G.; Gómez, D. Metal fractionation of atmospheric aerosols via sequential chemical extraction: A review. *Anal. Bioanal. Chem.* **2005**, *381*, 302–316. [CrossRef]

22. Li, H.; Wang, J.; Wang, Q.; Qian, X.; Qian, Y.; Yang, M.; Li, F.; Lu, H.; Wang, C. Chemical fractionation of arsenic and heavy metals in fine particle matter and its implications for risk assessment: A case study in Nanjing, China. *Atmos. Environ.* **2015**, *103*, 339–346. [CrossRef]

23. Manousakas, M.; Papaefthymiou, H.; Eleftheriadis, K.; Katsanou, K. Determination of water-soluble and insoluble elements in PM2.5 by ICP-MS. *Sci. Total Environ.* **2014**, *493*, 694–700. [CrossRef] [PubMed]

24. Canepari, S.; Pietrodangelo, A.; Perrino, C.; Astolfi, M.L.; Marzo, M.L. Enhancement of source traceability of atmospheric PM by elemental chemical fractionation. *Atmos. Environ.* **2009**, *43*, 4754–4765. [CrossRef]

25. Tessier, A.; Campbell, P.G.C.; Bisson, M. Sequential Extraction Procedure for the Speciation of Particulate Trace Metals. *Anal. Chem.* **1979**, *51*, 844–851. [CrossRef]

26. Muntau, H.; Quevauviller, P.; Griepink, B. Speciation of heavy metals in soils and sediments an account of the improvement and harmonization of extraction techniques undertaken under the auspices of the bcr of the commission of the european communities. *Int. J. Environ. Anal. Chem.* **1993**, *51*, 135–151. [CrossRef]

27. Chester, R.; Lin, F.J.; Murphy, K.J.T. A three stage sequential leaching scheme for the characterisation of the sources and environmental mobility of trace metals in the marine aerosol. *Environ. Technol. Lett.* **1989**, *10*, 887–900. [CrossRef]

28. Zatka, V.J.; Stuart Warner, J.; David, M. Chemical Speciation of Nickel in Airborne Dusts: Analytical Method and Results of An Interlaboratory Test Program. *Environ. Sci. Technol.* **1992**, *26*, 138–144. [CrossRef]

29. Kyotani, T.; Iwatsuki, M. Determination of Water and Acid Soluble Components in Atmospheric Dust by Inductively Coupled Plasma Atomic Emission Spectrometry, Ion Chromatography and Ion-Selective Electrode Method. *Anal. Sci.* **1998**, *14*, 741–748. [CrossRef]

30. Heal, M.R.; Hibbs, L.R.; Agius, R.M.; Beverland, I.J. Total and water-soluble trace metal content of urban background PM 10, PM2.5 and black smoke in Edinburgh, UK. *Atmos. Environ.* **2005**, *39*, 1417–1430. [CrossRef]

31. Conca, E.; Malandrino, M.; Giacomino, A.; Costa, E.; Ardini, F.; Inaudi, P.; Abollino, O. Optimization of a sequential extraction procedure for trace elements in Arctic PM10. *Anal. Bioanal. Chem.* **2020**, *412*, 7429–7440. [CrossRef]

32. Wang, G.; Wang, H.; Yu, Y.; Gao, S.; Feng, J.; Gao, S.; Wang, L. Chemical characterization of water-soluble components of PM10 and PM2.5 atmospheric aerosols in five locations of Nanjing, China. *Atmos. Environ.* **2003**, *37*, 2893–2902. [CrossRef]

33. Truzzi, C.; Annibaldi, A.; Illuminati, S.; Mantini, C.; Scarponi, G. Chemical fractionation by sequential extraction of Cd, Pb, and Cu in Antarctic atmospheric particulate for the characterization of aerosol composition, sources, and summer evolution at Terra Nova Bay, Victoria Land. *Air Qual. Atmos. Health* **2017**, *10*, 783–798. [CrossRef]

34. Canepari, S.; Cardarelli, E.; Perrino, C.; Catrambone, M.; Pietrodangelo, A.; Strincone, M. Two-stage chemical fractionation method for the analysis of elements and non-volatile inorganic ions in PM10 samples: Application to ambient samples collected in Rome (Italy). *Atmos. Environ.* **2006**, *40*, 7908–7923. [CrossRef]

35. Kyotani, T.; Iwatsuki, M. Characterization of soluble and insoluble components in PM_2.5 and PM10 fractions of airborne particulate matter in Kofu city, Japan. *Atmos. Environ.* **2002**, *36*, 639–649. [CrossRef]

36. Illuminati, S.; Annibaldi, A.; Truzzi, C.; Libani, G.; Mantini, C.; Scarponi, G. Determination of water-soluble, acid-extractable and inert fractions of Cd, Pb and Cu in Antarctic aerosol by square wave anodic stripping voltammetry after sequential extraction and microwave digestion. *J. Electroanal. Chem.* **2015**, *755*, 182–196. [CrossRef]

37. Illuminati, S.; Bau, S.; Annibaldi, A.; Mantini, C.; Libani, G.; Truzzi, C.; Scarponi, G. Evolution of size-segregated aerosol mass concentration during the Antarctic summer at Northern Foothills, Victoria Land. *Atmos. Environ.* **2016**, *125*, 212–221. [CrossRef]

38. Illuminati, S.; Annibaldi, A.; Bau, S.; Scarchilli, C.; Ciardini, V.; Grigioni, P.; Girolametti, F.; Vagnoni, F.; Scarponi, G.; Truzzi, C. Seasonal Evolution of Size-Segregated Particulate Mercury in the Atmospheric Aerosol over Terra Nova Bay, Antarctica. *Molecules* **2020**, *25*, 3971. [CrossRef]

39. PNRA Meteo-Climatological Observatory of the Italian National Antarctic Research Programme (PNRA). Available online: http://www.climantartide.it (accessed on 15 June 2020).

40. Yang, K.X.; Swami, K.; Husain, L. Determination of trace metals in atmospheric aerosols with a heavy matrix of cellulose by microwave digestion-inductively coupled plasma mass spectroscopy. *Spectrochim. Acta Part B* **2002**, *57B*, 73–84. [CrossRef]

41. Swami, K.; Judd, C.D.; Orsini, J.; Yang, K.X.; Husain, L. Microwave assisted digestion of atmospheric aerosol samples followed by inductively coupled plasma mass spectrometry determination of trace elements. *Anal. Bioanal. Chem.* **2001**, *369*, 63–70. [CrossRef] [PubMed]

42. Canepari, S.; Cardarelli, E.; Giuliano, A.; Pietrodangelo, A. Determination of metals, metalloids and non-volatile ions in airborne particulate matter by a new two-step sequential leaching procedure. Part A: Experimental design and optimisation. *Talanta* **2006**, *69*, 581–587. [CrossRef]

43. Harron, D.W.G. Technical Requirements for Registration of Pharmaceuticals for Human Use: The ICH Process. In *The Textbook of Pharmaceutical Medicine*; Wiley: Hoboken, NJ, USA, 2005.

44. Hans Wedepohl, K. The composition of the continental crust. *Geochim. Cosmochim. Acta* **1995**, *59*, 1217–1232. [CrossRef]

45. Tuncel, G.; Aras, N.K.; Zoller, W.H. Temporal variations and sources in the South Pole atmosphere. 1. Nonenriched and moderately enriched elements. *J. Geophys. Res.* **1989**, *94*, 13025–13038. [CrossRef]

46. Stein, A.F.; Draxler, R.R.; Rolph, G.D.; Stunder, B.J.B.; Cohen, M.D.; Ngan, F. Noaa's hysplit atmospheric transport and dispersion modeling system. *Bull. Am. Meteorol. Soc.* **2015**, *96*, 2059–2077. [CrossRef]

47. Nguyen, H.D.; Riley, M.; Leys, J.; Salter, D. Dust storm event of February 2019 in Central and East Coast of Australia and evidence of long-range transport to New Zealand and Antarctica. *Atmosphere* **2019**, *10*, 653. [CrossRef]

48. Mezgec, K.; Stenni, B.; Crosta, X.; Masson-Delmotte, V.; Baroni, C.; Braida, M.; Ciardini, V.; Colizza, E.; Melis, R.; Salvatore, M.C.; et al. Holocene sea ice variability driven by wind and polynya efficiency in the Ross Sea. *Nat. Commun.* **2017**, *8*. [CrossRef] [PubMed]

49. Caiazzo, L.; Baccolo, G.; Barbante, C.; Becagli, S.; Bertò, M.; Ciardini, V.; Crotti, I.; Delmonte, B.; Dreossi, G.; Frezzotti, M.; et al. Prominent features in isotopic, chemical and dust stratigraphies from coastal East Antarctic ice sheet (Eastern Wilkes Land). *Chemosphere* **2017**, *176*, 273–287. [CrossRef]

50. Artaxo, P.; Andrade, F.; Maenhaut, W. Trace elements and receptor modelling of aerosols in the antarctic peninsula. *Nucl. Inst. Methods Phys. Res. B* **1990**, *49*, 383–387. [CrossRef]

51. Artaxo, P.; Rabello, M.L.C.; Maenhaut, W.; Grieken, R. VAN Trace elements and individual particle analysis of atmospheric aerosols from the Antarctic peninsula. *Tellus B* **1992**, *44*, 318–334. [CrossRef]

52. Fan, S.; Gao, Y.; Sherrell, R.M.; Yu, S.; Bu, K. Concentrations, particle-size distributions, and dry deposition fluxes of aerosol trace elements over the Antarctic Peninsula in austral summer. *Atmos. Chem. Phys.* **2021**, *21*, 2105–2124. [CrossRef]

53. Gao, Y.; Xu, G.; Zhan, J.; Zhang, J.; Li, W.; Lin, Q.; Chen, L.; Lin, H. Spatial and particle size distributions of atmospheric dissolvable iron in aerosols and its input to the Southern Ocean and coastal East Antarctica. *J. Geophys. Res. Atmos.* **2013**, *118*, 12634–12638. [CrossRef]

54. Illuminati, S.; Annibaldi, A.; Truzzi, C.; Mantini, C.; Conca, E.; Malandrino, M.; Giglione, G.; Fanelli, M.; Scarponi, G. Determination of Cd, Pb, and Cu in the Atmospheric Aerosol of Central East Antarctica at Dome C (Concordia Station). *Molecules* **2021**, *26*, 1997. [CrossRef] [PubMed]

55. Winton, V.H.L.; Dunbar, G.B.; Atkins, C.B.; Bertler, N.A.N.; Delmonte, B.; Andersson, P.S.; Bowie, A.; Edwards, R. The origin of lithogenic sediment in the south-western Ross Sea and implications for iron fertilization. *Antarct. Sci.* **2016**, *28*, 250–260. [CrossRef]

56. Dick, A.L. Concentrations and sources of metals in the Antarctic Peninsula aerosol. *Geochim. Cosmochim. Acta* **1991**, *55*, 1827–1836. [CrossRef]

57. Wagenbach, D.; Gorlach, U.; Moser, K.; Munnich, K.O. Coastal Antarctic aerosol: The seasonal pattern of its chemical composition and radionuclide content. *Tellus B* **1988**, *40 B*, 426–436. [CrossRef]

58. Mishra, V.K.; Kim, K.H.; Hong, S.; Lee, K. Aerosol composition and its sources at the King Sejong Station, Antarctic peninsula. *Atmos. Environ.* **2004**, *38*, 4069–4084. [CrossRef]

59. López-García, P.; Gelado-Caballero, M.D.; Collado-Sánchez, C.; Hernández-Brito, J.J. Solubility of aerosol trace elements: Sources and deposition fluxes in the Canary Region. *Atmos. Environ.* **2017**, *148*, 167–174. [CrossRef]

60. Hueglin, C.; Gehrig, R.; Baltensperger, U.; Gysel, M.; Monn, C.; Vonmont, H. Chemical characterisation of PM2.5, PM10 and coarse particles at urban, near-city and rural sites in Switzerland. *Atmos. Environ.* **2005**, *39*, 637–651. [CrossRef]

61. Duan, J.; Tan, J. Atmospheric heavy metals and Arsenic in China: Situation, sources and control policies. *Atmos. Environ.* **2013**, *74*, 93–101. [CrossRef]

62. Dallarosa, J.; Calesso Teixeira, E.; Meira, L.; Wiegand, F. Study of the chemical elements and polycyclic aromatic hydrocarbons in atmospheric particles of PM10 and PM2.5 in the urban and rural areas of South Brazil. *Atmos. Res.* **2008**, *89*, 76–92. [CrossRef]

63. Lanzaco, B.L.; Olcese, L.E.; Querol, X.; Toselli, B.M. Analysis of PM2.5 in Córdoba, Argentina under the effects of the El Niño Southern Oscillation. *Atmos. Environ.* **2017**, *171*, 49–58. [CrossRef]

64. Richter, P.; Griño, P.; Ahumada, I.; Giordano, A. Total element concentration and chemical fractionation in airborne particulate matter from Santiago, Chile. *Atmos. Environ.* **2007**, *41*, 6729–6738. [CrossRef]

65. Chan, Y.C.; Simpson, R.W.; Mctainsh, G.H.; Vowles, P.D.; Cohen, D.D.; Bailey, G.M. Source apportionment of PM2.5 and PM10 in Brisbane (Australia) by receptor modelling. *Atmos. Environ.* **1999**, *33*, 3251–3268. [CrossRef]

66. Venter, A.D.; Van Zyl, P.G.; Beukes, J.P.; Josipovic, M.; Hendriks, J.; Vakkari, V.; Laakso, L. Atmospheric trace metals measured at a regional background site (Welgegund) in South Africa. *Atmos. Chem. Phys.* **2017**, *17*, 4251–4263. [CrossRef]

67. Jiang, S.Y.N.; Yang, F.; Chan, K.L.; Ning, Z. Water solubility of metals in coarse PM and PM2.5 in typical urban environment in Hong Kong. *Atmos. Pollut. Res.* **2014**, *5*, 236–244. [CrossRef]
68. Cheng, M.C.; You, C.F.; Cao, J.; Jin, Z. Spatial and seasonal variability of water-soluble ions in PM 2.5 aerosols in 14 major cities in China. *Atmos. Environ.* **2012**, *60*, 182–192. [CrossRef]
69. Sholkovitz, E.R.; Sedwick, P.N.; Church, T.M.; Baker, A.R.; Powell, C.F. Fractional solubility of aerosol iron: Synthesis of a global-scale data set. *Geochim. Cosmochim. Acta* **2012**, *89*, 173–189. [CrossRef]
70. Baker, A.R.; Jickells, T.D.; Witt, M.; Linge, K.L. Trends in the solubility of iron, aluminium, manganese and phosphorus in aerosol collected over the Atlantic Ocean. *Mar. Chem.* **2006**, *98*, 43–58. [CrossRef]
71. Sedwick, P.N.; Sholkovitz, E.R.; Church, T.M. Impact of anthropogenic combustion emissions on the fractional solubility of aerosol iron: Evidence from the Sargasso Sea. *Geochem. Geophys. Geosyst.* **2007**, *8*, 8. [CrossRef]
72. Jickells, T.D.; An, Z.S.; Andersen, K.K.; Baker, A.R.; Bergametti, C.; Brooks, N.; Cao, J.J.; Boyd, P.W.; Duce, R.A.; Hunter, K.A.; et al. Global iron connections between desert dust, ocean biogeochemistry, and climate. *Science* **2005**, *308*, 67–71. [CrossRef]
73. Xu, G.; Chen, L.; Zhang, M.; Zhang, Y.; Wang, J.; Lin, Q. Year-round records of bulk aerosol composition over the Zhongshan Station, Coastal East Antarctica. *Air Qual. Atmos. Health* **2019**, *12*, 271–288. [CrossRef]
74. Thamban, M.; Thakur, R.C. Trace metal concentrations of surface snow from Ingrid Christensen Coast, East Antarctica—Spatial variability and possible anthropogenic contributions. *Environ. Monit. Assess.* **2013**, *185*, 2961–2975. [CrossRef] [PubMed]
75. Grotti, M.; Soggia, F.; Ardini, F.; Magi, E. Major and trace element partitioning between dissolved and particulate phases in Antarctic surface snow. *J. Environ. Monit.* **2011**, *13*, 2511–2520. [CrossRef] [PubMed]
76. Grotti, M.; Soggia, F.; Ardini, F.; Magi, E.; Becagli, S.; Traversi, R.; Udisti, R. Year-round record of dissolved and particulate metals in surface snow at Dome Concordia (East Antarctica). *Chemosphere* **2015**, *138*, 916–923. [CrossRef]
77. Pongratz, R.; Heumann, K.G. Production of methylated Mercury, Lead and Cadmium by marine bacteria as a significant natural source for atmospheric heavy metals in polar regions. *Chemosphere* **1999**, *39*, 89–102. [CrossRef]
78. Planchon, F.A.; Boutron, C.F.; Barbante, C.; Cozzi, G.; Gaspari, V.; Wolff, E.W.; Ferrari, C.P.; Cescon, P.; Wol, E.W.; Ferrari, C.P.; et al. Changes in heavy metals in Antarctic snow from Coats Land since the mid-19th to the late-20th century. *Earth Planet. Sci. Lett.* **2002**, *200*, 207–222. [CrossRef]
79. Illuminati, S.; Annibaldi, A.; Romagnoli, T.; Libani, G.; Antonucci, M.; Scarponi, G.; Totti, C.; Truzzi, C. Distribution of Cd, Pb and Cu between dissolved fraction, inorganic particulate and phytoplankton in seawater of Terra Nova Bay (Ross Sea, Antarctica) during austral summer 2011–12. *Chemosphere* **2017**, *185*, 1122–1135. [CrossRef] [PubMed]
80. Corami, F.; Capodaglio, G.; Turetta, C.; Soggia, F.; Magi, E.; Grotti, M. Summer distribution of trace metals in the western sector of the Ross Sea, Antarctica. *J. Environ. Monit.* **2005**, *7*, 1256–1264. [CrossRef] [PubMed]
81. Bargagli, R.; Skotnicki, M.L.; Marri, L.; Pepi, M.; Mackenzie, A.; Agnorelli, C. New record of moss and thermophilic bacteria species and physico-chemical properties of geothermal soils on the northwest slope of Mt. Melbourne (Antarctica). *Polar Biol.* **2004**, *27*, 423–431. [CrossRef]
82. Ilyinskaya, E.; Oppenheimer, C.; Mather, T.A.; Martin, R.S.; Kyle, P.R. Size-resolved chemical composition of aerosol emitted by Erebus volcano, Antarctica. *Geochem. Geophys. Geosyst.* **2010**, *11*, 1–14. [CrossRef]
83. Boutron, C.F.; Patterson, C.C. Relative levels of natural and anthropogenic lead in recent Antarctic snow. *J. Geophys. Res.* **1987**, *92*, 8454–8464. [CrossRef]
84. Mcconnell, J.R.; Maselli, O.J.; Sigl, M.; Vallelonga, P.; Neumann, T.; Anschütz, H.; Bales, R.C.; Curran, M.A.J.; Das, S.B.; Edwards, R.; et al. Antarctic-wide array of high-resolution ice core records reveals pervasive lead pollution began in 1889 and persists today. *Sci. Rep.* **2014**, *4*, 4–7. [CrossRef] [PubMed]
85. Stohl, A.; Sodemann, H. Characteristics of atmospheric transport into the Antarctic troposphere. *J. Geophys. Res. Atmos.* **2010**, *115*, 115. [CrossRef]